

Behaviour of Shallow Foundations Subjected to Blast Loads and Related Liquefaction

Sangroya Ritika¹⁾ · Deepankar Choudhury¹⁾ · Young Jin Park²⁾ · Eun Chul Shin[†]

Received: July 25th, 2017; Revised: August 2nd, 2017; Accepted: August 31st, 2017

ABSTRACT : In recent years, world has witnessed many man-made activities related to both above and underground blasts. Details on behaviour of shallow foundations subjected to blast loads and induced liquefaction is scarce in literature. In this paper, typical shallow strip foundation in saturated cohesionless soils subjected to both above and underground blasting have been simulated by using finite difference based numerical model FLAC3D. Peak particle velocity (PPV) has been obtained to propose critical values for which bearing capacity failure for shallow foundations with soil liquefaction can occur. Typical results for pore pressure ratio (PPR) for various scaled distances are compared to PPR values obtained by using empirical equation available in literature which shows good agreement. Critical design values obtained in the present study for PPV and PPR to estimate the scaled distance, bearing capacity failure and liquefaction susceptibility can be used effectively for design of shallow strip foundation in cohesionless soil subjected to both above and under ground blast loads.

Keywords : Foundations, Blast, Liquefaction, FLAC, PPV, PPR

1. Introduction

Blasting is extensively carried out in mining operations, quarrying, and construction as well as for demolition of structures etc. Also, recently, bombing and missile attacks by terrorists have reported serious damage to structures. Owing to very small duration and very high pressure, blasting can have great influence on the stability of a structure: super-structure together with sub-structure. This is particularly important in defense engineering where storage of explosive weapons in underground is a common practice. Blast induced vibrations are particularly studied in free field condition. But if, blasting occurs close to foundation, effect of blasting on bearing capacity cannot be neglected. In addition, where water-table exists within the vicinity of foundation, susceptibility of foundation soil to liquefy also becomes important. Therefore design of foundation needs to be revised under such conditions. Inclusion of blast loads in dynamic analysis is today's necessity for foundation design. However, very limited research has been carried out in this area.

Some researchers have analyzed field data and derived empirical formulae for displacement, velocity, acceleration,

pore pressure ratio, compressive strains etc. under blast loads. Drake & Little (1983) had carried out analysis of field data, to provide formulae for estimating blast pressure and blast-induced vibrations. However one cannot directly use those empirical formulae for foundation design subjected to blast loading because soil structure interaction will play major role. Siskind & Stagg (1985) have done experimental work to study the blast-induced vibrations of foundations. Charlie et al. (2005) carried out centrifuge and prototype tests to find out blast-induced stress wave propagation and attenuation in soil media.

Analysis of field blast tests shows that propagation of waves in cohesive soils is greatly affected by presence of water if saturation is 95% or more (Drake & Little, 1983). Increase in peak stresses and acceleration was observed in wet clays, clay shale and sandy clays compared to dry condition. In contained explosion, water bearing sands behave mechanically as liquids and that's why only shock waves with steep front can propagate through them. Drake & Little (1983) also noted that granular soils with high relative density are comparatively less influenced by water saturation under blasting. However saturated sands with lower relative density

1) Department of Civil Engineering, Indian Institute of Technology Bombay, India

2) Department of Civil and Environmental Engineering, Incheon National University

† Department of Civil and Environmental Engineering, Incheon National University (Corresponding Author : ecshin@inu.ac.kr)

produce similar effects as cohesive soils. Few researchers evaluated the explosion induced pore water pressure to find out the scaled distance (ratio of distance from the blast source to the cube root of weight of the explosion) up to which liquefaction and ground mounding occurred (Veyera, 1985; Charlie et al., 1983; Charlie et al., 1996). Recently Kumar et al. (2012) had reviewed and shown the need for such study. Also Sangroya & Choudhury (2013) had shown the effective use of finite difference based geotechnical software FLAC3D (2006) for modeling the behaviour of soil slope subjected to blast loads in side a tunnel.

In the present study, numerical model of strip foundation in saturated soil subjected to both above and underground blasting are prepared using finite difference program FLAC3D (Fast Lagrangian Analysis of Continua) and the effects have been studied by determining the variation of peak particle displacement and velocity with scaled distance, reduction of bearing capacity of foundations and generation of excess pore water pressure. FLAC3D is well suited for modeling nonlinear systems (Itasca Consulting Group, 1999). The program adapts the dynamic equations of motion so as to ensure a stable numerical scheme when the physical system being modeled is unstable (Itasca Consulting Group, 1999). Other researchers did the blast resistant analysis for tunnel by using numerical modeling in FLAC2D (Olofsson et al., 1999) but it had limitations related to two dimensional (2D) analysis. Hence in the present study, three dimensional (3D) model has been simulated.

2. Calibration of FLAC^{3D} for blast load in free field

FLAC3D is an explicit finite difference program, which performs Lagrangian analysis and is best suited for geotechnical analysis in soils and rocks. FLAC3D enables to simulate full-scale model due to the availability of third dimension. In order to study the response of shallow foundations to blast loads, many factors, such as, fixity conditions, in-situ stresses, damping values need to be calibrated. It is done by comparing the radial velocities of soil subjected to blasting in free field condition with FLAC2D values and empirical values from CONWEP program (Olofsson et al., 1999) as well as velocities obtained using scalar wave equation

(Blake, 1952).

Olofsson et al. (1999) calibrated and compared FLAC2D model with idealized field data. Explosion effects due to bombs were obtained from CONWEP program based on field data compiled by U.S Army. Properties of field soil (Moraine soil) was defined by density of 1,900 kg/m³ and seismic velocity of 1,000 m/s. Rayleigh damping was applied, where the damping matrix is proportional to mass and stiffness of the system.

In the present study, the grid for soil is generated using meshing with the cubical element shape to reduce the computational time. The origin of axis coincides with the center of detonation point. When an underground explosion takes place, the initial zone of excitement of the soil approaches the shape of sphere (Barkan, 1962). Hence a sphere is modeled using FISH function, which is built-in programming language to define our own equation. Blast pressure is applied on the surface of sphere. Sensitive analysis was performed to choose the finer mesh in the region near the blasting to capture the accurate measurement and the coarse mesh in other regions to optimize the running time of model. The 'fix' command is used to prevent the change of velocity or displacement at selected points. Base of the model is restrained for horizontal and vertical movement, and sides of model are restrained only for horizontal displacements. Soil is assumed to behave elastically. To simulate crater due to blast, 'FISH' function is used to form mirrored quarter spheres. Blast load was applied using FISH function 'wave', where the blast pressure raised linearly up to peak pressure 7.336 MPa, thereby decreasing exponentially with time. Figure 1 shows FLAC3D model as per site layout considered in the present study.

FLAC uses viscous boundary scheme, consisting of two sets of dashpots attached independently to the mesh in normal and shear directions. Hence it absorbs the propagating waves at the model boundaries and reduces the reflections of blast wave into the model. Artificial viscous damping was provided for the transient blast wave propagation. The purpose of this is to diffuse the shock wave front over an increased number of zones as wave progresses and damp the oscillations behind the front. Radial velocity was found by using velocities in x-direction, y-direction and z-direction. Table 1 shows that FLAC3D values are within range of radial velocities, which were obtained from FLAC2D, CONWEP and mathematical formula for spherical propagation in solid medium by Blake.

Table 1. Validation and comparison of radial velocities (m/s) in free field blast condition

Point	FLAC2D (Olofsson et al., 1999)	CONWEP (Olofsson et al., 1999)	Blake (1952)	FLAC3D (Present Study)
P1	2.65	3.93	2.05	2.94
P3	1.00	0.62	0.81	1.10
P5	2.10	1.67	1.54	1.43

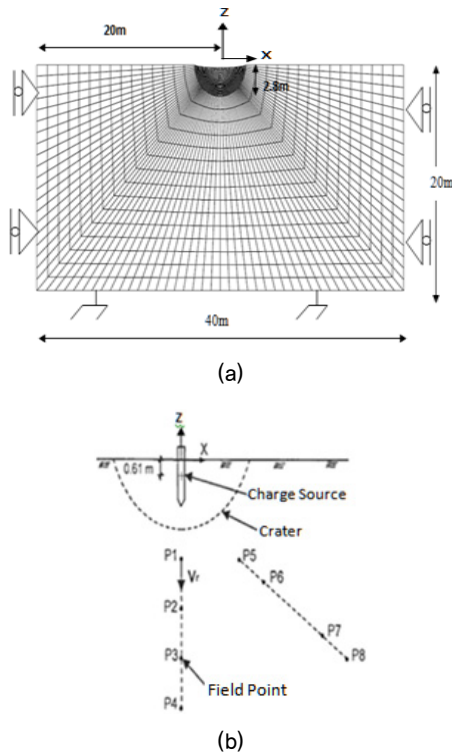


Fig. 1. (a) FLAC3D model showing soil with crater with boundary and fixity conditions, (b) Location of field points relative to center of charge (modified after Olofsson et al., 1999)

Thus, elastic model with viscous damping, fixity and in-situ conditions, as stated, satisfactorily simulates blasting in free-field conditions.

3. Numerical modeling

Numerical analysis has been found to be suited for analyzing blast induced liquefaction below strip foundation with large deformations because the complicated transient loading, boundary conditions and soil behavior could be modeled. FLAC3D enables the full scale simulation especially in case of blasting where vibrations in third dimension do add up to final velocity and displacement.

3.1 Model definition

The model contains two groups/units; soil and footing. Footing load applied at the embedment depth produces stress contours exactly as they are formed below a shallow footing. Figure 2 shows the strip footing considered in the present study. B and D_f are width and depth of footing respectively. R is the radius of sphere at which blast pressure is applied. 'z' is the depth of blast point. Using technical reasoning like boundary of pressure bulb with less than 10% stress at ground level and the extent of possible failure surface with trial and error method to eliminate effects of boundaries on the model, size of model considered is $25\text{ m} \times 10\text{ m} \times 10\text{ m}$. To apply under ground blast load, aspherical cavity of radius 0.5 m is modeled by using FISH function for user-defined variables.

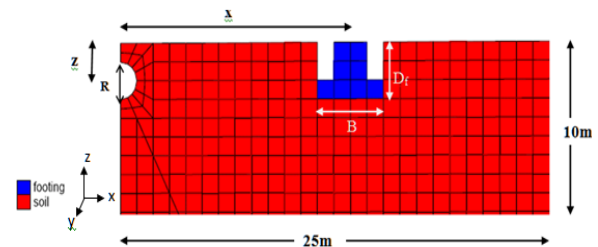


Fig. 2. Typical FLAC3D model studied for embedded shallow strip footing in cohesionless soil

It is assumed to be small strains due to vibrations, hence elastic model is sufficient as it saves running time. Properties used are cohesion, friction, density, bulk modulus, shear modulus, tensile strength, permeability and porosity. After the grid is generated, boundary and initial conditions are applied. Boundaries are fixed in the respective normal directions. This is to keep the model in equilibrium so that zero shear stresses are produced at the boundaries. Initial stresses are only the self weight due to gravity and velocities are zero at the beginning.

3.2 Soil properties

Field stresses due to gravity are initialized. Allowable load is estimated by using closed form equation of Terzaghi's bearing capacity (Bowles, 1982). Before applying the blast load, model is brought to the state of equilibrium. Only the dry density of soil needs to be given as an input, FLAC3D calculates the wet density once the dry density, water density and porosity of soil are introduced. In the present study,

drainage is not permitted in order to simulate the behavior of foundation for worst condition- undrained condition. Other important input parameters used are bulk modulus, density, permeability.

Analysis is carried out for sandy soils in saturated conditions. Table 2 gives the properties used in present study. Equation 1 gives ultimate bearing capacity (q_u) of strip footing in homogeneous cohesionless soil.

$$q_u = \frac{1}{2} \gamma B S_\gamma N_\gamma + \gamma D_f S_q N_q \quad (1)$$

where, γ is the unit weight of soil; B is width of footing; D_f is the embedment depth of the footing; S_γ , S_q are the shape factors; N_γ and N_q are Meyerhof's bearing capacity factors for cohesionless soil.

Table 3 shows the foundation properties of strip footing and

Table 2. Foundation soil properties used in the present study (Bowles, 1982)

Property	Type of soil	
	Dense sand	Loose sand
Cohesion c_u (kPa)	0	0
Friction angle ϕ' (°)	38o	28o
Unit weight γ_{dry} (kN/m ³)	8.05	14.42
Relative density (%)	80	35
Poisson's ratio (ν) (dry)	0.3	0.4
Poisson's ratio (ν) (saturated)	0.45	0.45
Young's modulus (MPa)	33-58	18-24
Porosity	0.31	0.45
Coefficient of permeability (m/s)	1×10^{-5}	1×10^{-3}

Table 3. Foundation properties of strip footing, bearing capacity with blast input parameters (as per TM5-855-1) considered in the present study for different cohesionless soils

Soil type		Dense sand	Loose sand
Geometry	B	2.0	2.0
	L	20	20
	D_f (m)	1.5	1.5
Bearing capacity (kPa)		658	46
Seismic wave velocity, c (m/s)		1,500	2.5
Attenuation coefficient, n		500	2.5
Acoustic impedance, $\rho_c \times 10^3$ (Ns/m ³)		32.25	9.60
Coupling factor, f		0.75	0.75
Arrival time (t_a) at $R=0.5$ m (ms)		0.33	1.00

bearing capacity of homogeneous cohesionless soil considered in the present analysis.

Simulation of foundation can be understood from the contours of stresses in z direction (SZZ) due to application of static bearing load and corresponding displacements in z direction below foundation in homogeneous cohesionless soil as shown in Figure 3.

3.3 Blast parameters

In the present study, both above and underground blast loads are considered to act on the chosen strip foundation. Blast-induced vibrations, reduction in bearing capacities and also liquefaction effects are studied to see how type of soils, distance between the point of explosion and center of foundation affects the stability of shallow foundation. The

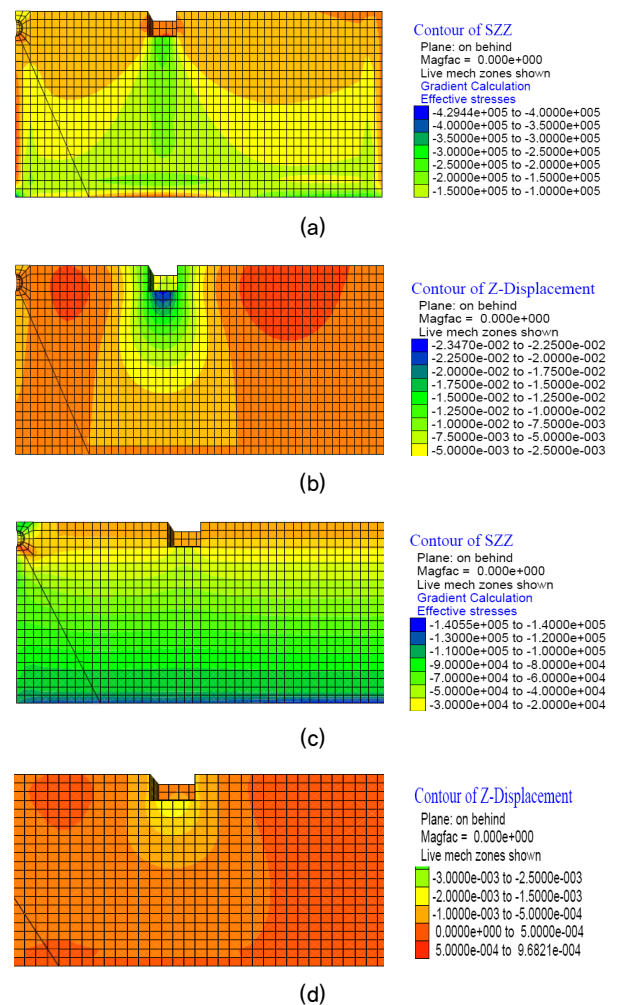


Fig. 3. (a) SZZ stress (N/m²) and (b) z-displacement (m) contours for strip footing insaturated dense sand (c) SZZ stress sand (d) z-displacement (m) contours for strip footing in saturated loose sand

main aim is to find out the critical scaled distance at which foundation will be just safe under various blast loads, which can be used effectively in the design.

3.3.1 Underground blasting

Man-made vibrations include both controlled and uncontrolled blasting. Demolition of structures and mining come under controlled blasting whereas terrorist activities like bombings come under uncontrolled blasting. When missiles struck the ground, they first penetrate to a depth depending on the surface material and geological material and then explode (Bulson, 1997).

Table 3 also gives the dynamic properties of the soils used to estimate the peak blast pressure (P_o) in psi using formula given by TM5-855-1 (Equation 2) (TM 5-855-1, 1986).

$$P_o = 160 f(\rho c) \left(\frac{R}{\sqrt[3]{W}} \right)^{-n} \quad \text{psi} \quad (2)$$

Seismic velocity (c) in fps gives the velocity with which compression and shear waves (absent in case of saturated soils) propagate from the source of blast. Seismic velocity is the lowest for dry loose sand and the highest for dense sand because it depends on the inter-particle packing and bonding. As inter-particle bonding and packing is higher in dense sand, hence seismic velocity is also higher compared to that in loose sand. Attenuation coefficient (n) gives the

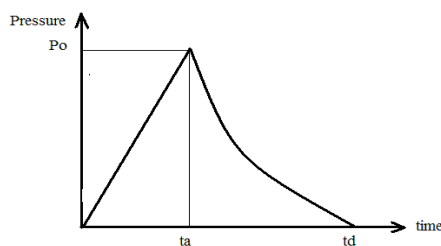


Fig. 4. Blast pressure-time histories with P_o as peak pressure, t_a as arrival time and t_d as damped time

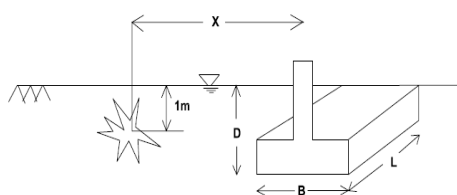


Fig. 5. Schematic diagram showing underground blasting point and shallow strip footing

rate at which blast pressure will reduce. Slight intrusion of air attenuates blast pressure at a faster rate. Acoustic impedance (ρc) gives the absorbing capacity of soil. It is the product of density (ρ) in lb/ft^3 and seismic velocity (c). Coupling factor (f) gives the fraction of blast energy that is transferred to soil. Greater the depth of blast source, higher will be the coupling factor. For scaled depths greater than $1.4 \text{ m/kg}^{1/3}$, coupling factor is constant at 1. R is the scaled depth and W is weight of TNT blast. Arrival time (t_a) of blast wave at any distance is estimated by dividing the distance by seismic velocity. It was assumed that the blast pressure on the sphere of radius 0.5 m increases linearly up to peak value as per Equation 2 and the n declines exponentially. Figure 4 gives the typical blast pressure versus time history.

Figure 5 shows the schematic diagram of underground blasting. Indian code IS: 6922-1973 (1973) gave a guideline for safety criteria of structures subjected to underground blast loads which needs to be considered for design.

In reality, underground blasting will be bound by free-surface. Depth of the blast was kept constant at a depth of 1 m and 'X' which is the distance of center of footing from blast point was varied from 4 m to 20 m. Free field pressure was multiplied by 1.5 considering the presence of structure below ground level (Yang, 1997).

3.3.2 Aboveground blasting

Vehicular bombings, tragic severe accidents with explosion etc. pose serious threat to the integrity of whole structure. In case of above ground blast, a part of energy is in the form of thermal radiation and remaining part as air pressure and ground shock. Here, the effect of 1,000 kg TNT explosive detonated above ground, on substructure is studied. Contact explosion which takes place at soil-air interface was considered since its yield is almost twice that of air explosion. In Figure

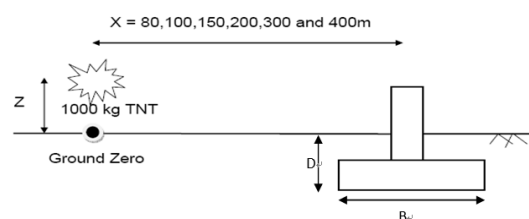
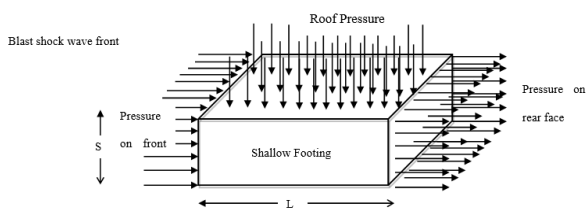


Fig. 6. Schematic diagram showing above ground blasting near shallow strip footings

6, z is the distance of blast point from ground surface, which is assumed to be zero for present analysis to study the most critical situation.

When an explosive charge is detonated in air, the loading can no longer be considered uniform and it is necessary to examine the spread and decay of instantaneous pressure pulse as it travels across external areas of a structure. Same holds true for substructure. Side-on overpressure versus time distribution for buried structures was calculated as per Figures 3 and 4 of Indian design code IS: 4991-1968 (1968). Scaled distances were restricted to $8 \text{ m/kg}^{1/3}$ since all foundations showed failure mechanism (reduction in bearing resistance or liquefaction) for distance of blasting 80 m from center of footing for 1,000 kg explosive i.e. scaled distance of $8 \text{ m/kg}^{1/3}$. Front-face was assumed to be the face of footing nearer to point of blasting while rear-face was assumed to be the face away from point of blasting. Roof was assumed to be the top face of footing. As the two remaining sides of footing were not perpendicular to the blast wave propagation (least affected), pressure on sides was assumed to be negligible. Figure 7 shows pressure application on different faces of footing.

Table 4 gives an overview of side-on overpressure applied for shallow footings at scaled distances $10 \text{ m/kg}^{1/3}$ to $40 \text{ m/kg}^{1/3}$ from ground zero. It is calculated from the side-on



Note: L is distance from face nearer to blast point up to face farther from blast point

Fig. 7. Pressure distributions on footing for various faces of buried structures as per IS-4991-1968 (1968)

Table 4. Side-on Overburden Pressure (Pso) values versus scaled distance as per IS-4991-1968 (1968)

Scaled distance ($\text{m/kg}^{1/3}$)	Side-on pressure (Pso) in Pa	Damped time (td) in milliseconds
10	1513683.0	3.92
15	784800.0	5.39
20	379254.6	8.61
30	118700.0	17.00
40	80268.3	19.53

over pressure versus time distribution for buried structure as per Indian design code IS-4991-1968 (1968). Damped time is the equivalent triangular wave pulse time as defined in IS-4991-1968.

4. Results and discussions

In the present study, failure of strip foundation in saturated soil under blast loading is studied by determining the variation of peak particle velocity (PPV) with scaled distance, reduction in bearing capacity and generation of excess pore water pressure. Results for both above and underground blasting in saturated soils are discussed below.

4.1 Underground blasting in saturated soil

In this study, explosion in soil bounded by a free surface was considered. Blasting is modeled as TNT (Trinitrotoluene) explosive having blast energy of 4,680 kJ/kg and detonation velocity of 6,940 m/s. Figure 8 shows the variation of peak pressure against scaled distance for shallow strip footing in loose and dense sands.

Strip footing was subjected to these pressures. Footings were placed at various distances of 4 m to 20 m from detonation point. Results were compared with scaled distance ($\text{m/kg}^{1/3}$) for uniformity.

4.1.1 Reduction in resistance offered by foundation

The static bearing pressure applied to foundations acts as resistance to external loads. This resistance is affected due to blast load (Table 5). It was observed that SZZ (stress along z direction on plane having normal in z direction), which initially is the static bearing pressure changes as the

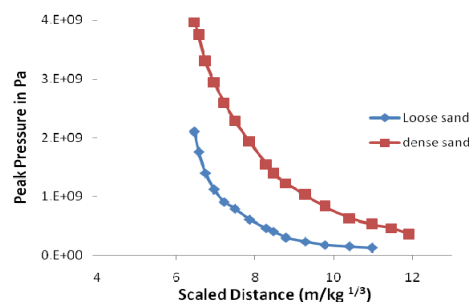


Fig. 8. Peak blast pressure for different saturated soils subjected to underground blast

Table 5. Reduced bearing resistance with scaled distance (SD) for strip footing

Scaled distance (m/kg ^{1/3})	Minimum normal stress (kPa) in z-direction (SZZ) below center of footing after blasting	
	Dense sand	Loose sand
6.93	355.0	0
7.21	368.0	0
15.00	480.0	6.7

blast load effect advances towards the footing. Increase in SZZ below the center of footing is followed by reduction and becoming equal to static pressure since elastic model is considered. Saturated soil behaves like ideal fluid when subjected to blast loads because of very high P-wave velocity.

4.1.2 Variation of PPV

For saturated soils, peak particle velocity (PPV) becomes the governing factor that controls liquefaction induction and finally the stability of foundation soil. Hence, in this case only the variation of PPV is given. Figure 9 shows PPV variation with scaled distance for strip footing in both loose and dense sands. It can be observed that both the soils have essentially same PPV at scaled distances greater than 20 m/kg^{1/3}.

4.1.3 Blast induced liquefaction

Blast induced residual pore pressures are produced by one or multiple cycles of compressive strains for repetitive loadings. Excess pore water pressures and residual pore pressure ratio (PPR) are used to predict liquefaction. Explosives detonated in water saturated soils produce high intensity compression waves which build high excess pore pressures that

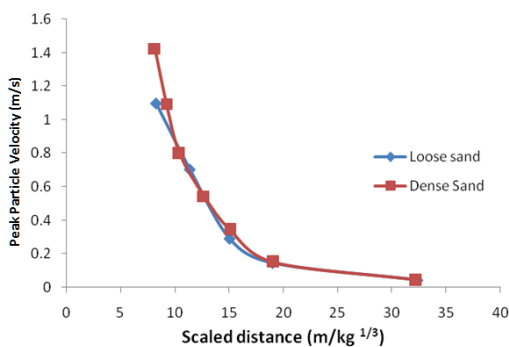


Fig. 9. Peak Particle Velocity (PPV) in m/s v/s scaled distance for different saturated soils with strip footing subjected to underground blast

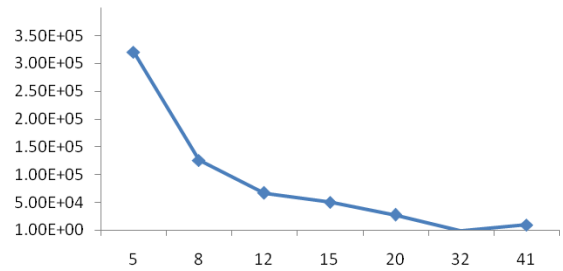


Fig. 10. Excess pore pressure (N/m²)v/s scaled distance (m/kg^{1/3}) for strip footings in saturated loose sand subjected to underground blast

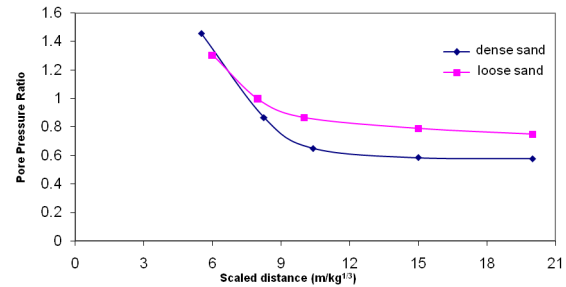


Fig. 11. PPR variations with scaled distance in loose and dense sand for shallow strip footing subjected to underground blast

may trigger liquefaction. Loose sand showed highest excess pore water pressure at any given scaled distance due to lower relative density. Figure 10 shows the excess pore water pressure with scaled distance.

Pore pressure ratio (PPR) is the ratio of excess pore water pressure to initial effective stress, it is also residual pore water pressure divided by initial total stress. Figure 11 shows variation of PPR with the scaled distance for both loose and dense sands. As expected, loose sand shows significantly higher PPR than that for dense sand at higher scaled distance.

4.2 Above ground blasting in saturated soil

1,000 kg TNT explosive is exploded at distances 80 m, 100 m, 150 m, 200 m, 300 m and 400 m from the centre of footing. Reduction in bearing resistance and blast-induced liquefaction are the major effects of ground surface blast on strip footings in saturated soils.

4.2.1 Reduction in resistance offered by foundation

On application of ground blast load, SZZ sharply increases to a large significant value and then reduces sometimes even reaching zero, indicating zero resistance obtained from foundation to the external load. Table 6 shows reduced SZZ

Table 6. Reduced bearing resistance (SZZ) at the center of footings in saturated soils

Scaled distance (m/kg ^{1/3})	Minimum (bearing stress in z-direction) SZZ, below footing (kPa)	
	Dense sand	Loose sand
10	474.9	0
15	535.4	10.6
20	546.3	36.0

values at center of footing for strip footing in saturated soils. Strip footing in loose sand failed early, at scaled distance of 10 m/kg^{1/3}.

4.2.2 Variation of PPV and PPD

Foundation in loose sand shows higher peak particle velocity than foundation in dense sand. Figure 12 shows the variation of PPD (peak particle displacement) and PPV with scaled distance for different types of soil.

4.2.3 Blast induced liquefaction

Aboveground blasting generates sudden increase in pore

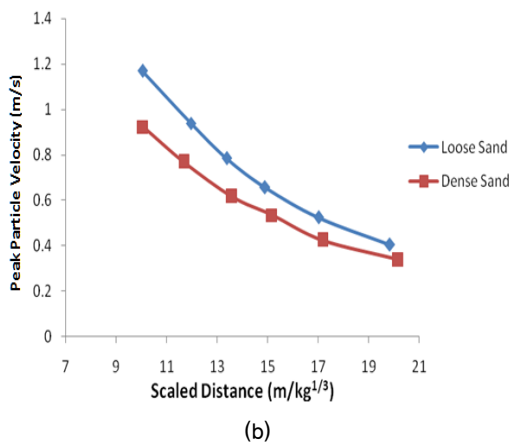
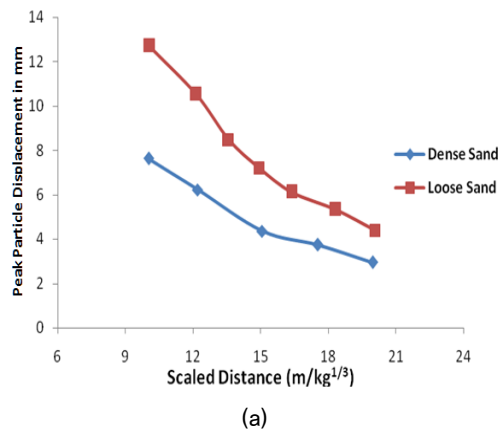


Fig. 12. Variation of (a) PPD and (b) PPV with scaled distance for strip footing in saturated loose and dense sands subjected to aboveground blast

pressure that can cause liquefaction in cohesion less soil. Table 7 gives excess pore pressure for strip footings in saturated soils.

Loose sands show higher excess pore pressure than dense sand. Table 8 shows PPR for strip footings in saturated loose and dense sand. For loose sands, foundations show susceptibility to liquefaction at all studied cases of scaled distance as PPR is greater or close to 1.

Table 9 shows the scaling distances at which strip foundation fails and PPV at which soil just liquefied for different types of cohesionless soils for both underground and above ground blasting.

4.3 Validation of PPR with results of Veyera

From field tests, Veyera proposed a semi-empirical formula

Table 7. Excess pore pressure (kPa) below center of footing in saturated soils for aboveground blasting

Scaled distance (m/kg ^{1/3})	Dense sand	Loose sand
10	921	1026
15	301	423
20	82	201

Table 8. Pore Pressure Ratio (PPR) for shallow strip footing in saturated cohesionless soils subjected to aboveground blasting

Scaled distance (m/kg ^{1/3})	Pore pressure ratio (PPR)	
	Dense sand	Loose sand
8	>1.000	>1.000
10	>1.000	>1.000
15	>1.000	>1.000
20	0.808	>1.000
30	-	>1.000
40	-	0.952

Note: '-' indicates not feasible/not carried out

Table 9. Critical values of parameters for failure of shallow strip foundation in saturated cohesionless soil subjected to both underground blasting and above ground blasting

Type of soil	Scaled distance at which bearing resistance fails (m/kg ^{1/3})	PPV at which bearing resistance fails (m/s)	PPV at which soil is just liquefied (m/s)
For underground blasting			
Dense sand	10.40	1.600	1.500
Loose sand	6.93	0.651	0.651
For aboveground blasting			
Dense sand	8.0	1.12	0.52
Loose sand	10.0	1.16	0.16

Table 10. Comparison of values of pore pressure ratio (PPR) obtained from semi-empirical formula of Veyera and from present FLAC3D study

Scaled distance (m/kg ^{1/3})	Values of PPR		% Difference
	by Veyera	by FLAC3D (Present Study)	
5.039	1.004	1.021	1.69
6.000	1.080	1.271	17.74
7.560	0.898	0.842	6.24
8.000	0.963	0.995	3.32
8.617	0.644	0.545	15.37
10.000	0.889	0.865	2.70
10.080	0.790	0.700	11.39
12.600	0.735	0.727	1.09
12.920	0.547	0.472	13.71
15.000	0.790	0.789	0.13
17.230	0.510	0.432	15.29
18.890	0.617	0.664	7.62
20.000	0.720	0.749	4.03
21.544	0.471	0.422	10.40
25.190	0.590	0.534	9.49
32.310	0.402	0.400	0.50
43.080	0.283	0.331	17.10

to calculate pore pressure ratio (PPR) from peak particle velocity (PPV), relative density and initial effective stress, as given by,

$$PPR = 6.7(PPV)^{0.33} (\sigma')^{-0.31} (D_r)^{-0.179} \quad (3)$$

Where, PPV is peak particle velocity in m/s, σ' is effective overburden pressure in kN/m² i.e. bearing pressure in case of footing and D_r is the relative density which is considered in the present study for looses and =35%. PPR at a point depends on the amount of blast energy and how far that point is from source of detonation.

Table 10 shows comparison of values of PPR obtained from semi-empirical formula (Veyera, 1985) and that obtained in the present study for underground blasting using FLAC 3D. Maximum difference of 17.74% is observed in case of liquefied soil. Figure 13 shows that the values of Pore Pressure Ratio (PPR) for strip footing as obtained for loose sand subjected to under ground blast using FLAC3D in the present analysis is a revery close to the PPR calculated by using semi-empirical formula proposed by Veyera. It indicates that FLAC3D results can be effectively used to estimate PPR for various scale distances of blast loading.

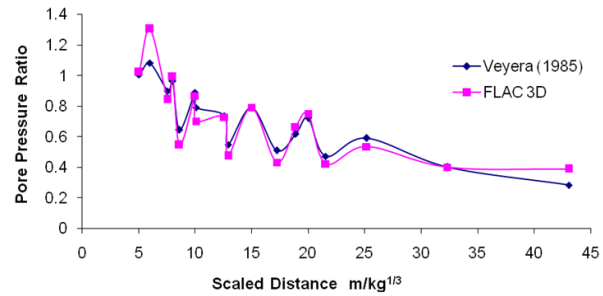


Fig. 13. Comparison of Pore Pressure Ratio (PPR) for strip footing in loose sand subjected to underground blast using FLAC3D with semi-empirical formula by Veyera

5. Conclusions

The present study has described the necessity of considering both underground and aboveground blast loads on shallow strip foundation. It has been observed that the bearing capacity reduces significantly under both types of blast loadings depending on the type of cohesionless soil. To find out the safest distance of the foundation within different types of cohesionless soils from charge source, results for peak particle velocity (PPV) and peak particle displacement (PPD) values are determined at various scaled distances. In both cases of underground and aboveground blasting, pore pressure ratio (PPR) is directly proportional to PPV. Also it is observed that PPR is inversely proportional to bearing capacity. In saturated soils, inferior performance is observed in case of loose sand, with strip footing failing for bearing resistance at scaled distance of about 15 m/kg^{1/3} with PPV values of 0.55 m/s~0.9 m/s. FLAC3D found to be effective finite difference based numerical method of model such shallow strip footing under blast loads to obtain the response in terms of stress and displacements. Also the significant effect of blast loads for inducing liquefaction in the cohesionless soil is observed. Typical results obtained shows the needy range to consider for design of shallow strip footing under effective scaled distance to consider the blast load effects on reduced bearing capacity and liquefaction of cohesionless soil. It is observed that typically PPV of 0.16 m/s can induce liquefaction below strip foundation in saturated loose sands. Footing fails at higher values of scaled distance for under ground blasting as compared to above ground blasting in case of dense sand, and vice versa for shallow strip footing in loose sand. Present results found to be in good agreement with that proposed by earlier researcher using semi-empirical

formula for estimation of PPR. Hence present results, mainly the critical values of the scaled distance and PPV at which bearing capacity failure occurs and PPV at which liquefaction occurs can be effectively used for design of shallow strip footings in cohesionless soils under both underground and above ground blast loads.

References

1. Barkan, D. D. (1962), Dynamics of bases and foundations, McGraw Hill Book Company, New York, pp. 390-414.
2. Blake, F. G. (1952), Spherical wave propagation in solid media, The Journal of Acoustical Society of America, 24, No. 2, pp. 211-215.
3. Bowles, J. E. (1982), Foundation analysis and design, McGraw Hill Book Company, ISBN 0-07-006770-8, pp. 968-996.
4. Bulson, P. S. (1997), Explosive loading of engineering structures, Taylor and Francis e-library, ISBN-0-203-78210, p. 236.
5. Charlie, W. A., Veyera, G. E., Abt, S. R. and Patrone, H. D. (1983), Blast induced soil liquefaction – State-of-the-Art, Proceedings of Symposium in The Interaction of Non-Nuclear Munitions with Structure, Part II, pp. 62-68.
6. Charlie, W. A., Veyera, G. E., Durnford, D. S. and Doehring, D. O. (1996), Pore pressure increases in soil and rock from underground chemical and nuclear explosions, Engineering Geology, 43, pp. 225-236.
7. Charlie, W. A., Dowden, W. A., Villano, E. J., Veyera, G. E. and Doehring, D. O. (2005), Blast-induced stress wave propagation and attenuation: centrifuge model versus prototype tests, Geotech. Test. J. ASTM, 28, No. 2, pp. 1-10.
8. Drake, J. L. and Little C. D. (1983), Ground shock from penetrating conventional weapons, The Interaction of Non-Nuclear Munitions with Structures: Symposium Proceedings, Part I, pp. 1-6.
9. FLAC3D (2006), Fast langragian analysis of continua in 3Dimensions, Version 3.1, User's Manual Itasca Consulting Group, Minneapolis, Minnesota, USA, pp. 44-53.
10. IS-4991-1968 (1968), Criteria for blast resistant design of structures or explosions above ground, Indian Standard, New Delhi, pp. 4-7.
11. IS-6922-1973 (1973), Criteria for safety and design of structures subjected to underground blast, Indian Standard, New Delhi pp. 5-8.
12. Kumar, R., Choudhury, D. and Bhargava, K. (2012), Response of foundations subjected to blast loadings: State of the art review, Disaster Advances, 5, No. 1, pp. 54-63.
13. Olofsson S. O., Rosengren L. and Svedbjork, G. (1999), Modeling of ground- shock wave propagation in Soil Using FLAC, FLAC and Numerical Modeling in Geomechanics, Detournay and Hart ed., A.A Balkema Publishers, Rotterdam, Netherlands, pp. 401-405.
14. Sangroya, R. and Choudhury, D. (2013), Stability analysis of soil slope subjected to blast induced vibrations using FLAC3D, Proceedings of Geo-Congress – 2013, Stability and Performance of Slopes and Embankments III, Geotechnical Special Publication, ASCE, March 3-6, 2013, San Diego, CA, USA, p. 472.
15. Siskind, D. E. and Stagg, M. S. (1985), Blast vibration measurements near and on structure foundations, Bureau of Mines, Report of Investigations, 8969, pp. 1-20.
16. TM 5-855-1 (1986), Fundamentals of protective design for conventional weapons, U.S. Department of the Army, Vicksburg, Mississippi, pp. 16-19.
17. Veyera, G. E. (1985), Transient pore water pressure response and liquefaction in a saturated sand, Ph.D. Dissertation Colorado State University, Dept. of Civil Engineering, Ft. Collins, CO, USA, pp. 209-215.
18. Yang, Z. (1997), Finite element simulation of response of buried shelters to blast loading, Finite Elements in Analysis and Design, 24, pp. 113-132.